Geometry and topology of knotted ring polymers in an array of obstacles

Enzo Orlandini[1,2], Attilio L. Stella[1,2], and Carlo Vanderzande[3,4]
[1] *Dipartimento di Fisica and CNR-INFM, Università di Padova, I-35131, Padova, Italy.*
[2] *Sezione INFN, Università di Padova, I-35131 Padova, Italy.*
[3] *Departement WNI, Hasselt University, 3590 Diepenbeek, Belgium.*
[4] *Instituut Theoretische Fysica, Katholieke Universiteit Leuven, 3001 Heverlee, Belgium.*
(Dated: November 12, 2010)

We study knotted polymers in equilibrium with an array of obstacles which models confinement in a gel or immersion in a melt. We find a crossover in both the geometrical and the topological behavior of the polymer. When the polymers' radius of gyration, R_G, and that of the region containing the knot, $R_{G,k}$, are small compared to the distance b between the obstacles, the knot is weakly localised and R_G scales as in a good solvent with an amplitude that depends on knot type. In an intermediate regime where $R_G > b > R_{G,k}$, the geometry of the polymer becomes branched. When $R_{G,k}$ exceeds b, the knot delocalises and becomes also branched. In this regime, R_G is independent of knot type. We discuss the implications of this behavior for gel electrophoresis experiments on knotted DNA in weak fields.

PACS numbers: 36.20.Ey, 87.15.A-, 02.10.Kn

Circular DNA, as found in bacteria and phages, is often knotted [1]. Such knots are produced by the action of enzymes known as topoisomerases or by random cyclization inside the head of a phage [2]. Investigation of the types of knots produced can give important insights in the working of these processes. The knot type of a single DNA can be determined from electron or atomic force microscopy. When large numbers of knotted rings have to be analysed one uses gel electrophoresis [3]. One expects that for a fixed number of basepairs (bp), a DNA with larger minimal crossing number n_c [4] will have a smaller radius and hence a higher mobility under weak electric field. This expectation is verified experimentally [5] but despite extensive work [6] the precise relation between mobility and knot complexity is not fully understood. For example, the dependence on the length of the DNA, as measured by the number of basepairs, has not been clarified yet.

The behavior of melts of polymers of various architecture (linear, branched, ring) is also of high interest [7]. In [8], the geometrical and dynamical properties of an *unknotted* ring polymer in an array of obstacles were studied. The array was used as a model for a gel but the results were also considered to be relevant for melts of ring polymers. Indeed, in a recent experiment [9], the relaxation spectrum predicted in [8] was observed in a melt of ring polystyrenes. However, since these polymers were synthesized near theta conditions, they can contain knots [10]. This is thus another situation in which topological and geometrical constraints may simultaneously affect the behavior of a polymer.

Finally, in the crowded environment of a cell, the average size of a macromolecule is often larger than the average distance between macromolecules, leading, e.g., to important effects on kinetics and geometry of proteins [11]. Since some proteins are also knotted [12] it is of interest to understand how their topological properties are modified in crowded *in vivo* situations.

Here we study the behavior of a *single* knotted and self-avoiding ring polymer in a regular, cubic, array of obstacles with lattice constant b. Besides being a model of a gel or melt, such regular arrays can also be realised experimentally using hydrogels [13] and in microfluidics [14, 15], where they have been used to separate DNA.

In this Letter, we clarify how the excluded volume constraints exerted by the presence of an array of obstacles affect the geometrical behaviors of knotted ring polymers in equilibrium. The novel insight concerning knot localization [16] and topology dependence of the size of the rings will be valuable for the interpretation of gel electrophoresis of knotted DNA in weak fields.

Knotted polymer rings are modelled as N edges self-avoiding polygons [17] on the cubic lattice. Each edge corresponds to one persistence length. In the case of DNA this length equals approximately 50 nm or 150 bp. For an agarose gel, in which most of the experiments with (knotted) DNA are performed, the size of the holes is of the order of 200 to 500 nm [3]. In our model, this corresponds to a b-value from 4 to 10. In the microlitographic arrays of ref. [14], the effective pore size of 1μm corresponds to $b \approx 20$. Vertices occupied by obstacles, and the edges connecting them, are not available for the polygons. This constraint will decrease the overall entropy of the polygons with respect to the free space case affecting both their overall conformational equilibrium properties and the typical size of the knotted portion.

The equilibrium properties of the polygons are studied by Monte Carlo simulations based on BFACF, topology preserving moves [18]. This algorithm works in a grand canonical ensemble where configurations are weighted with a step fugacity K [17]. The average number of monomers N will diverge when the fugacity approaches a critical value K_c, which is related to the entropy per monomer $s = -k_B \ln K_c$ [17]. To increase the Monte

Carlo efficiency we implement the BFACF algorithm on to a multiple Markov chain sampling scheme [19] using several values of $K < K_c$. K_c depends strongly on the confining geometry and, for each value of b an exploratory simulation has to be done in order to estimate $K_c(b)$. In free space, $K_c = 0.213538$. We determined $K_c(b = 10) = 0.2227, K_c(b = 7) = 0.2318$ and $K_c(b = 5) = 0.2515$. As expected $K_c(b)$ increases as b decreases since for smaller values of the lattice constant b, obstacles are more dense in space, the confinement of the polymers is stronger and hence the entropy s is lower. We perform our simulations up to K-values slightly below $K_c(b)$, which allows us to study self-avoiding polygons of several thousand steps, which in the DNA-context correspond with molecules of a few hundred kbp, a regime in which self-avoidance effects cannot be neglected.

We next determined the average mean squared radius of gyration $\langle R^2 \rangle$ as a function of binned N-values independently of the K-value at which polygons of a given knot type were generated. We expect $\langle R^2 \rangle \sim N^{2\nu}$. In three-dimensional free space, $\nu = \nu_f = 0.589$. The polymer should begin to 'feel' the presence of the obstacles when its typical size $R_G = \langle R^2 \rangle^{1/2}$ becomes of the order of b. When R_G/b is small, we should recover the behavior in absence of obstacles. If on the other hand R_G/b is sufficiently large, a new regime dominated by the obstacles should appear. Fig. 1 shows our data for $\langle R^2 \rangle / b^2$ as a function of $x = N/g$ where g is the number of monomers in one b-cell, $R(N = g) \equiv b$. For large b this gives $g \sim b^{1/\nu_f}$ so that $x = N/b^{1/\nu_f}$ follows. The results refer to the trefoil knot ($n_c = 3$). The data for various b-values collapse on a single curve, which can be fitted as a combination of two straight lines, the slopes of which are respectively $2\nu = 1.15 \pm 0.02$ and $2\nu = 0.99 \pm 0.02$. The

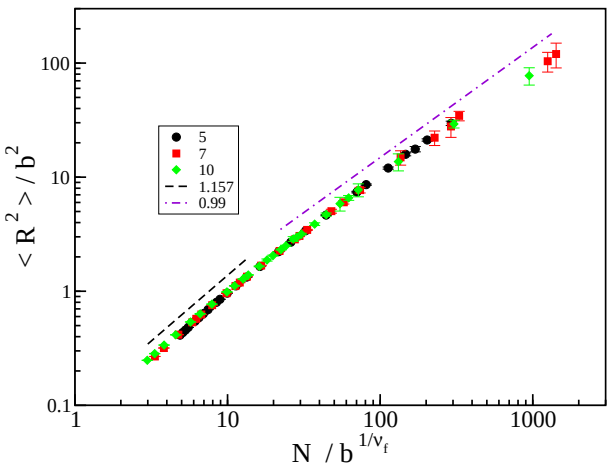

FIG. 1: (Color online) Log-log plot of $\langle R^2 \rangle / b^2$ as a function of $x = N/b^{1/0.589}$ for three b-values (results for trefoil knot). The dashed line has a slope 1.16, the dot-dashed one 1.00.

former value agrees with $2\nu_f$. The latter is well consistent with that for self-avoiding branched polymer (BP) in $d = 3$ for which $\nu_{BP} = 1/2$ [20, 21] (Fig. 2). The crossover that we find here was never observed before. It occurs around $x = x_c \approx 20$. Fig. 1 clearly shows that at the crossover, $R_G \approx b$.

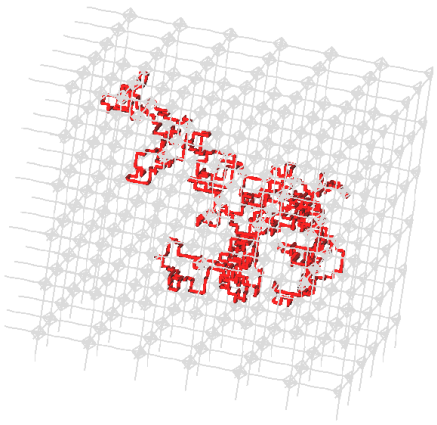

FIG. 2: (Color online) Branched polygon with a composite $3_1 \sharp\, 3_1$ knot in an array with $b = 7$.

Another important property of knotted polymers is the size l_k of the knotted region. Intuitively it corresponds to the minimal number of monomers that still contain the topological entanglement of the knot. Research in the last decade has clearly shown that l_k [16, 22] is a fluctuating quantity whose statistical properties strongly depends on the physical conditions of the polymer [23]. In good solvent, it was found that a knot is weakly localized. This means that the average number of monomers in the knot $\langle l_k \rangle$ grows as a power of N, $\langle l_k \rangle \sim N^t$, with an exponent $t < 1$ [16]. Numerically, one has $t \simeq 0.75$. In contrast, in the collapsed globular phase, the knot delocalizes ($t = 1$) [16, 24].

For the knotted polymer inside the array of obstacles we determined l_k using the 'cut and join'-algorithm presented in [16]. In Fig. 3, we report $\langle l_k \rangle / b^{1/\nu_f}$ as a function of x for the trefoil and for different b-values. The results collapse once more on one curve. Moreover, there is again a crossover between two regimes. In the first one, the knot is weakly localised with an exponent that we estimate as $t = 0.69 \pm 0.04$, consistent within error bars, with the value in good solvent [16]. At higher x, the exponent $t = 1.05 \pm 0.15$ indicates *delocalization* of the knot.

This delocalisation crossover occurs at a higher value of x than that of the geometrical crossover, namely $x = x_d \approx 100$. This suggest that the delocalisation of the knot only occurs when the average squared radius of gyration of the knotted region, $\langle R_k^2 \rangle$ becomes of the order of b^2. In Fig. 4 we have therefore plotted $\langle R_k^2 \rangle / b^2$ versus $\langle l_k \rangle / b^{1/\nu_f}$. These results indeed show that the knotted

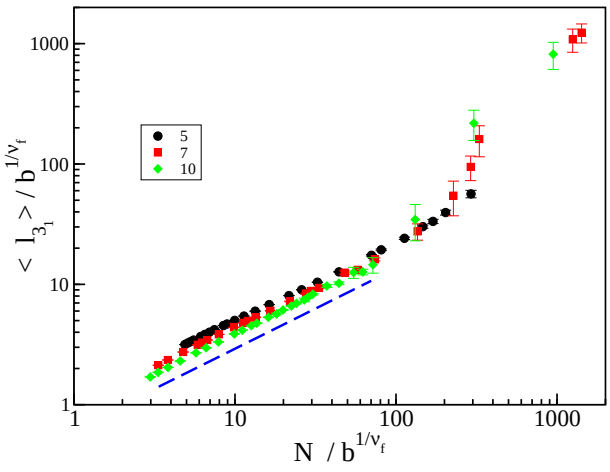

FIG. 3: (Color online) Log-log plot of the mean length of the trefoil knot, $\langle l_{3_1}\rangle$, scaled by b^{1/ν_f} as a function of x for three b-values. The dashed line has a slope 0.69.

region behaves in a way completely similar to the whole polymer: once $R_{G,k} = \langle R_k^2\rangle^{1/2}$ becomes equal to the distance between the obstacles, its geometry changes from self-avoiding to branched. Comparing Fig. 3 and Fig. 4, we see that the knot indeed delocalises when $R_{G,k}$ is close to b.

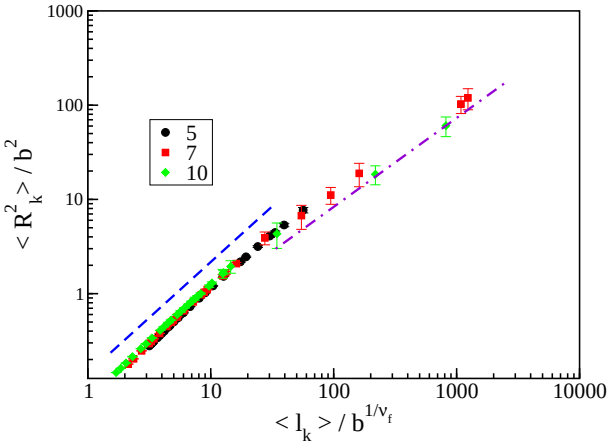

FIG. 4: (Color online) Log-log plot of $\langle R_k^2\rangle/b^2$ as a function of $\langle l_k\rangle/b^{1/0.589}$ for three b-values (results for trefoil knot). The dashed line has a slope 1.18, the dot-dashed one 0.98.

To summarize, there are three regimes for a knotted ring polymer in an array of obstacles. In the first regime the knot is weakly localised and geometrically both the knot and the whole polymer behave as in good solvent with $\nu = \nu_f$. The polymer is essentially confined in one single cell of the array of obstacles. In a second regime, for $20 < x < 100$, the polymer spreads over several cells but the knot is still confined to a single one. As a consequence the geometry of the whole polymer becomes branched, whereas the knotted part still behaves as in good solvent. In these two regimes, the knot is localised. Finally, for $x > 100$, the knot delocalises and assumes a branched shape just as the whole polymer.

We next investigated the dependence of our results on knot complexity by extending our calculations to the prime knots 4_1 and 6_1 and to the composite knot $3_1\sharp\, 3_1$ and, for comparison, to the unknot. For this study we fixed $b = 7$.

In Fig. 5 we present our results for $\langle R^2\rangle/N$ as a function of N for the various knot types. The curves should reach a constant in the BP-regime. This figure shows several interesting features. Firstly, one observes that for small N, the $\langle R^2\rangle$ depends on knot type. The higher n_c, the smaller is the polymer. This is a result similar to that found for ideal knots [25]. Secondly, since more complex knots are smaller they feel the presence of the obstacles only for larger N. Hence, x_c depends on n_c. Finally, one notices that in the BP-regime, polymer size hardly depends on knot complexity. This result is rather unexpected. Therefore in the BP-regime it is difficult to determine the knot topology from geometry. This in contrast to the good solvent regime where the part of the polymer occupied by the knot, as measured by $\langle l_k\rangle$, increases with knot complexity. Evidence for this can be seen in Fig. 6 where we plot $\langle l_k\rangle/l_{\min}$ versus N. Here, $l_{\min}$ is the minimal number of edges necessary to embed a given knot type in the cubic lattice. For the trefoil, the

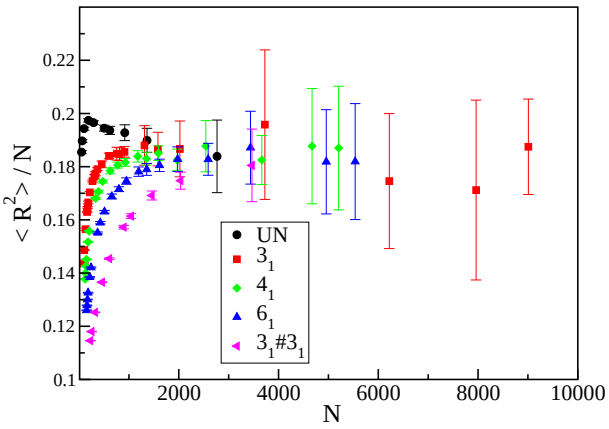

FIG. 5: (Color online) $\langle R^2\rangle/N$ versus N for different knot types in an array with $b = 7$.

4_1 and 6_1-knot, $l_{\min}$ equals respectively 24, 30 and 60 [26]. The data of Fig. 6 show that in the good solvent regime, $\langle l_k\rangle = C l_{\min} N^{0.69}$, where C is a knot-independent constant. This implies that the fraction of monomers in the knot, $\langle l_k\rangle/N$, increases with knot complexity.

Our results can have implications for gel electrophoresis experiments. Assuming as a first approximation that the knotted ring polymer is spherical with radius R_G, the mobility in a weak electric field $\mu \sim R_G^{-1}$, should

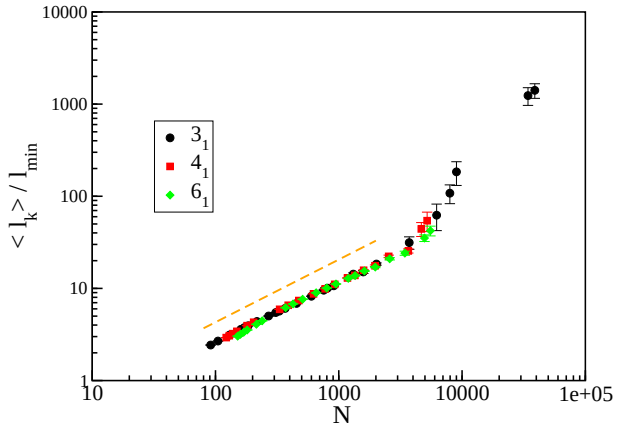

FIG. 6: (Color online) $\langle l_k \rangle / l_{\min}$ as a function of N for different knot types ($b = 7$). The dashed line has slope 0.69.

depend on knot type for small x-values. In this regime, different knot types can be separated by electrophoresis. However, our results predict that for x sufficiently large this is no longer possible. The precise value of x where this crossover occurs is model dependent and it is therefore not possible to predict at which N-values it should occur in real DNA. As an example, the genome of the P4-phage is an 11.6 kbp DNA which can contain different types of knots [2]. Its size has been estimated from atomic force microscopy to be about 300 nm [27]. This is of the same order as that of the holes in an agarose gel, so that x is of order one 1. Since these DNA's have been separated by electrophoresis, our results suggest that for somewhat longer knotted DNA's, the effects predicted here could be measurable. Microlithographic arrays of self-assembled magnetic beads [15] could also be used to reveal the crossovers.

Acknowledgement Support from the "Fondazione CARIPARO" within a "Progetto di Eccellenza" is acknowledged.

[1] A.D. Bates and A. Maxwell, *DNA Topology*, Oxford University Press (2005).
[2] J. Arsuaga, J. Vazquez, S. Trigueros, D. W. Sumners and J. Roca *Proc. Natl. Acad. Sci.* **99** 5373 (2002).
[3] J.-L. Viovy, *Rev. Mod. Phys.* **72** 813 (2000).
[4] D. Rolfsen, *Knots and links* (Wimington: Publish or Perish Press) (1976).
[5] A. Stasiak, Katritch V., Bednar J., Michoud D. and Dubochet J., *Nature* **384** 122 (1996).
[6] C. Weber, A. Stasiak, P. De Los Rios and G. Dietler, *Biophys. J.* **90** 3100 (2006).
[7] T. McLeish, *Phys. Today* **61** Issue 8, 40 (2008).
[8] S.P. Obukhov, M. Rubinstein and T. Duke, *Phys. Rev. Lett.* **73** 1263 (1994).
[9] M. Kapnistos *et al.*, *Nature Materials* **7 997** (2008).
[10] E. Orlandini and S.G. Whittington, *Rev. Mod. Phys.* **79**, 611 (2007).
[11] D. Homouz, M. Perham, A. Samiotakis, M.S. Cheung and P. Wittung-Stafshede, *Proc. Nat. Acad. Sci.* **105** 11754 (2008).
[12] W.R. Taylor, 2000 *Nature* **406** 916 (2000).
[13] L. Liu, P. Li and S.A. Asher, *Nature* **397** 141 (1999).
[14] W.D. Volkmuth and R.H. Austin, *Nature* **358** 600 (1992).
[15] P.S. Doyle, J. Bibette, A. Bancaud and J.-L. Viovy, *Science* **295** 2237 (2002).
[16] B. Marcone, E. Orlandini, A.L. Stella and F. Zonta, J. Phys. A **38**, L15 (2005); B. Marcone, E. Orlandini, A.L. Stella and F. Zonta, Phys. Rev. E **75**, 041105 (2007).
[17] C. Vanderzande, *Lattice models of polymers* (Cambridge University Press) (1998).
[18] B. Berg and D. Foester, *Phys. Lett.* **106B** 323 (1981); C. Aragao de Carvalhon, S. Caracciolo and J. Frohlich, *Nucl. Phys. B* **215** 209 (1983).
[19] M.C. Tesi, E.J. Janse van Rensburg, E. Orlandini and S.G. Whittington, *J. Stat. Phys.* **82** 155 (1996).
[20] G. Parisi and N. Sourlas, *Phys. Rev. Lett.* **46**, 871 (1981).
[21] The regime of ideal lattice animals for which $\nu = 1/4$ cannot be reached within our model which always includes self-avoidance.
[22] R. Metzler, A. Hanke, P.G. Dommersnes, Y. Kantor and M. Kardar *Phys. Rev. Lett.* **88** 188101 (2002).
[23] E. Orlandini, A.L. Stella and C. Vanderzande, *Phys. Biol.* **6** 025012 (2009).
[24] E. Orlandini, A.L. Stella and C. Vanderzande, Phys. Rev. E **68**, 031804 (2003); A. Hanke *et al.*, Eur. Phys. J. E **12**, 347 (2003).
[25] V. Katrich, J. Bednar, D. Michoud, R.G. Scharein, J. Dubochet and A. Stasiak, *Nature* **384**, 142 (1996).
[26] Y. Diao, *J. Knot Theory Ramif.* **2**, 413 (1993); E.J. Janse van Rensburg and S.D. Promislow, *J. Knot Theory Ramif.* **4**, 115 (1995).
[27] F. Valle, M. Favre, J. Roca and G. Dietler in *Physical and Numerical models in Knot theory* edited by J.A. Calvo, K.C. Millett, E.J. Rawdon and A. Stasiak (World Scientific) (2005).